

Article

Effects of Ball Size on the Grinding Behavior of Talc Using a High-Energy Ball Mill

Hyun Na Kim ^{1,*} , Jin Woo Kim ¹, Min Sik Kim ¹, Bum Han Lee ² and Jin Cheul Kim ²

¹ Department of Earth and Environmental Sciences, Kongju National University, Gongju 32588, Korea; ahop2000@kongju.ac.kr (J.W.K.); msms6365@smail.kongju.ac.kr (M.S.K.)

² Korea Institute of Geoscience and Mineral Resources, 124 Gwahak-ro, Yuseong-gu, Daejeon 34132, Korea; leebh@kigam.re.kr (B.H.L.); kjc76@kigam.re.kr (J.C.K.)

* Correspondence: hnkim@kongju.ac.kr; Tel.: +82-41-850-8513; Fax: +82-41-850-8953

Received: 26 September 2019; Accepted: 28 October 2019; Published: 31 October 2019



Abstract: The properties and preparation of talc have long been investigated due to its diverse industrial applications, which have expanded recently. However, its comminution behavior is not yet fully understood. Therefore, having better control of the particle size and properties of talc during manufacturing is required. In this study, we investigate the effect of the ball size in a high-energy ball mill on the comminution rate and particle size reduction. High-energy ball milling at 2000 rpm produces ultrafine talc particles with a surface area of 419.1 m²/g and an estimated spherical diameter of 5.1 nm. Increasing the ball size from 0.1 mm to 2 mm increases the comminution rate and produces smaller talc particles. The delamination of (001) layers is the main comminution behavior when using 1 mm and 2 mm balls, but both the delamination and rupture of (001) layers occurs when using 0.1 mm balls. The aggregation behavior of ground talc is also affected by the ball size. Larger aggregations form in aqueous solution when ground with 0.1 mm balls than with 1 mm or 2 mm balls, which highlights the different hydro-phobicities of ground talc. The results indicate that optimizing the ball size facilitates the formation of talc particles of a suitable size, crystallinity, and aggregation properties.

Keywords: nanoscale talc; wet milling; high-energy ball milling; ball size; aggregation

1. Introduction

Talc (Mg₃Si₄O₁₀(OH)₂) is a phyllosilicate mineral with a T-O-T layer composed of tetrahedral silicon and octahedral magnesium, which share oxygen and are strongly bonded with each other. The weak van der Waals bonds between the T-O-T layers is the origin of softness of talc. The silicon in the siloxane sheet renders talc hydrophobic, since it cannot easily be substituted with aluminum [1]. Talc is physically easy to handle due to low hardness, does not react with acid due to its chemical stability, and has high adsorptivity, low plasticity, and low thermal/electrical conductivity. Because of these characteristics, talc is used as a coating, refractory, and additive in various industrial fields such as paper, paint, rubber, ceramic, refractory material, and polymer manufacturing. Chemical and pharmaceutical industries also require high-grade talc powders with high purity and uniform particle sizes. The grade and usage of talc is classified considering the purity, whiteness, particle size, and more. For example, talc with a particle size of 44 μm is used in ceramics and paints, 8–12 μm in paper, 7 μm in cosmetics, and 2 μm or smaller in rubber [2]. In addition, the nanoscale talc recently received attention for its application in areas such as improving the heat resistance of nanocomposites, and for use in waste water filter materials [3–5].

Given the importance of the above, various attempts have been made to produce ultrafine talc powders and better understand their physicochemical properties [6–11]. Various processes, such as

planetary ball milling, tumbling milling, stirred ball milling, and disk milling, have been used to grind talc [10,12–17]. A reduction in particle size and the collapse of the crystalline structure of talc have been observed in mechanical grinding studies [8,10,12,13,15,18–20]. Table 1 summarizes the particle size and/or surface area of ground talc with processed various milling methods. Delamination of the layered structure in the direction of the (001) surface is the predominant mechanism of grinding, which, consequently, accompanies the breaking of individual plates and disordering in the talc crystal [8,10,15,21]. Further excessive grinding generally causes the collapse of the crystalline structure into the amorphous phase and the aggregation of ultrafine particles [13,14]. The degree of particle size reduction varies depending on the type of milling machine and milling conditions such as duration and rotating speed [11,21–26]. Besides the collapse of the crystalline structure, the physicochemical properties of talc such as thermal and dispersion behaviors, cation exchange capacity, wettability, and whiteness are also changed by mechanical grinding [6,10,12,14,27–29]. In accordance with the increasing demand for high-quality and ultrafine talc powder, the importance of comminution technology, capable of controlling crystallinity, particle shape, and particle size, is increasing.

Table 1. Specific surface area and equivalent spherical diameter of talc powder depending on the milling condition.

Milling Machine	Milling Type	Rotation Speed (rpm)	Grinding Time (h)	Ball Size (mm)	S.S.A. † (m ² /g)	ESD ‡ (nm)	D ₅₀ (µm)	References
Tumbling mill	dry	86	116.6	-	14.0	153	-	[13]
Planetary ball mill	dry	1350	0.5	16	10.5	204	-	[13]
Planetary ball mill	dry	-	0.5	-	109.7	20	-	[14]
Planetary ball mill	dry	-	5	-	28	76	-	[10]
Stirred ball mill	wet	2500	3.5	-	-	-	0.2	[17]
Stirred ball mill	dry	600	0.25	2.5–3.5	3.34	641	2.33	[16]
Disk mill	dry	70	6	-	17.3	128	-	[15]
High energy ball mill	wet	2000	12	2	419.1	5.1	0.37	This study
				1	365.1	5.9	0.44	
				0.1	171.7	12.5	7.96	

† S.S.A. = specific surface area. ‡ ESD = equivalent spherical diameter.

Planetary ball milling, which is one of the most frequently used lab-scale milling tools, has been applied to increase the grinding efficiency of talc. The collision impact and friction between powder samples and balls in a rotating jar grind the microscale talc into sub-microscale particles. The grinding efficiency of ball milling is greatly affected by the jar rotation speed, ball size, and ratio of balls and sample talc [22,24,25]. A faster rotation speed generally produces talc with a smaller particle size and lower crystallinity [11]. Recently developed high-energy ball mills reach rotation speeds of up to 2000 rpm and provide an opportunity to reduce the size of talc powder to the nanoscale level. The high-energy ball mill system consists of turn discs and jars. The oppositely rotating jar and turning disc produce highly energetic impact energy (Figure 1) [30]. However, while the ball size is an important factor in ball milling, the effect of the ball size on the comminution of talc has not yet been fully understood [31,32]. While the particle size is known to generally increase with an increasing ball size, in 2013, Shin et al. showed that particle size decreased and then increased as the ball size increased from 1 to 10 mm during the comminution of Al₂O₃ powder at low rotation speeds (50–153 rpm) [32]. The optimum ball size is dependent on the milling conditions and the properties of the mineral. Thus, to obtain ultrafine talc powder while minimizing the loss of crystallinity, a systematic approach is necessary to understand the effect of ball size in high-energy ball milling on the comminution of talc.

In this study, high-energy ball milling with high rotation speed of 2000 rpm is applied to obtain the nanoscale talc powder. The effect of the ball size for planetary ball milling on the grinding rate and behavior of talc is investigated with a varying ball size (2, 1, and 0.1 mm). Changes in the agglomeration characteristics of mechanochemical talc and the relationship with the ball size is also investigated.

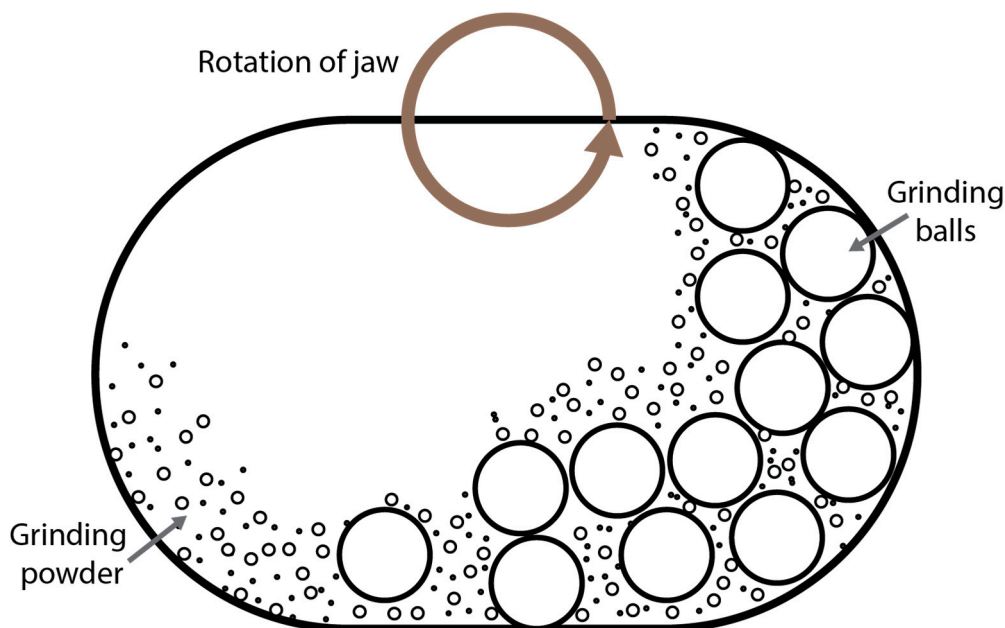


Figure 1. Schematic view of the motion of the balls and powder in a jar during high energy ball milling.

2. Materials and Methods

2.1. Sample Preparation

A commercial talc powder with high purity (>99%, XTA-400, KOCH corp., Shenyang, China) was used in this study. The mean particle size of an as-received powder is approximately 12 μm . The sample was mechanically deformed using a high-energy ball mill (Emax, Retsch, Haan, Germany), which generates ultrafine particles by combining impact and shear stress. Wet milling was performed by loading the talc powder, distilled water, and zirconia balls in the volume ratio of 2:3:4 into a 50 mL zirconia (ZrO_2) jar. Rotation speed was fixed at 2000 rpm and grinding time varied from 10 to 360 min. The time interval for grinding was selected by considering the trends in particle size and crystallinity of the talc following preliminary experiments. Zirconia balls of various sizes (2, 1, and 0.1 mm) were used. During grinding, the temperature of the milling jar was maintained at approximately 50 $^{\circ}\text{C}$ by a water-cooling system.

2.2. Characterization Methods

2.2.1. X-Ray Diffraction Analysis

X-ray diffraction (XRD) analysis was performed with the Rigaku SmartLab X-ray diffractometer (Rigaku, Tokyo, Japan) in the Korea Institute of Geoscience and Material Resources. $\text{Cu-K}\alpha$ radiation was used with a tube voltage of 40 kV and a current of 30 mA. The scan range was 3–90 $^{\circ}$ (2 θ) with an interval of 0.02 $^{\circ}$.

2.2.2. BET (Brunauer-Emmett-Teller) Specific Surface Area Analysis

The specific surface area of the talc sample was measured using the specific surface area analyzer (Micromeritics ASAP-2420, Norcross, GA, USA) in the Jeonju Center of Korea Basic Science Institute. Before the experiment, the adsorbed water on the talc particle surface was removed at 300 $^{\circ}\text{C}$ for 2 h, and then the BET method involving nitrogen adsorption method at 77 K was used.

2.2.3. Laser Diffraction Particle Size Analysis

The particle size was determined using a laser diffraction particle size analyzer (Mastersizer3000, Malvern Panalytical, Malvern, UK) in the Korea Institute of Geoscience and Material Resources. The talc in an aqueous colloid solution was dispersed for 10 min using a 28 kHz ultrasonic dispersing machine.

2.2.4. Scanning Electron Microscopy

Scanning electron microscopy was performed using the high-resolution scanning electron microscope (HR FE-SEM, TESCAN-MIRA3, Brno, Czech Republic) at the Kongju National University. The sample was coated with platinum (Pt) using an ion-coating machine at an accelerated voltage of 10.0 kV.

3. Results

3.1. X-Ray Diffraction Analysis

Figure 2 shows the XRD patterns of talc ground for up to 360 min using different ball sizes, which shows the effect of ball size on the crystallinity of ground talc.

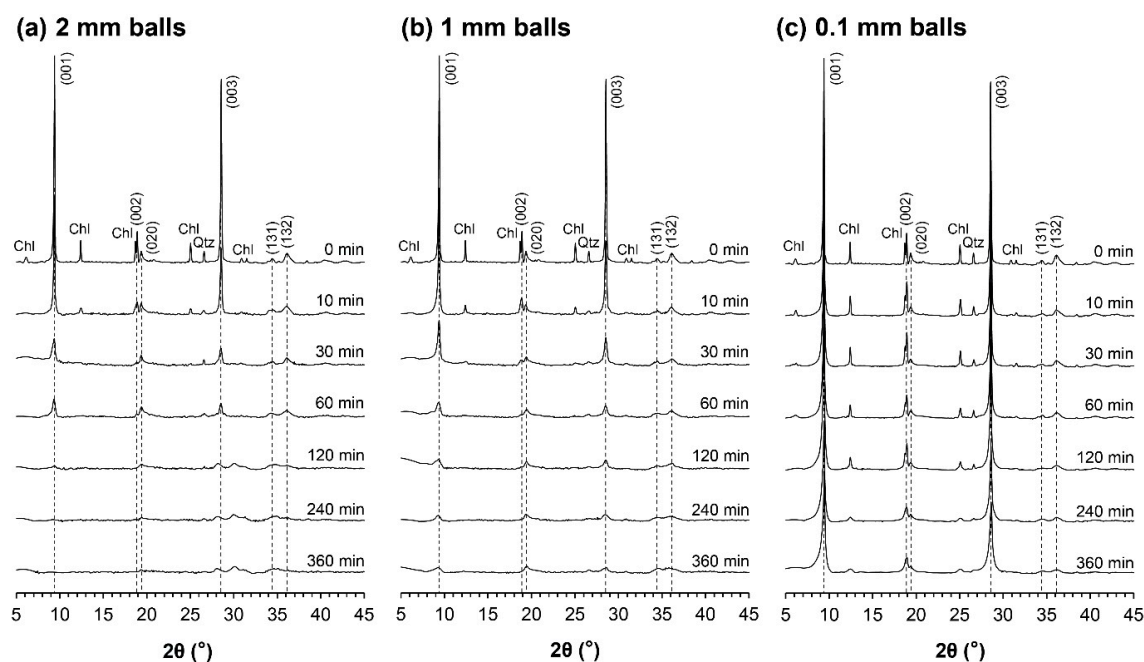


Figure 2. XRD patterns of talc powder upon grinding with (a) 2 mm, (b) 1 mm, and (c) 0.1 mm balls. Chl: chlorite, Qtz: quartz.

In the as-received talc, (001), (002), and (003) peaks of talc with a narrow width were observed at 2θ angles of 9.4° , 18.9° , and 28.6° , respectively [12]. The small peaks for chlorite and quartz were also observed, which were often found with talc as a result of carbonate alteration [33]. Upon grinding, the X-ray diffraction peak intensity gradually decreased while the peak width increased, which implied the decrease in crystallinity of ground talc. The degree and rate of reduction in peak intensity varies with the size of the balls used in grinding. When 2 mm or 1 mm balls were used for grinding, the peak intensity of the talc markedly decreased until 60 min of grinding. After 120 min of grinding, most diffraction peaks disappeared when the 2 mm balls were used. When 1 mm balls were used, small diffraction peaks were still observed, even though their intensities are very small compared with prior to grinding. A further change in the diffraction pattern was not observed for grinding by more than 120 min. These results indicated that ground talc for 120 min and more has a disordered or amorphous structure when 2 mm or 1 mm balls were used for grinding. When 0.1 mm balls were used, the decrease

in peak intensity was relatively sluggish. The peak intensity consistently decreased even after 120 min of grinding, which was in contrast with the cases using 2 mm or 1 mm balls. The unique diffraction pattern of talc was still apparent even after 360 min of grinding, which indicated a crystalline structure of talc left after grinding.

To quantitatively compare the effects of the ball size on the crystallinity of ground talc, the change in the relative height of the talc (001) peak, according to grinding, was analyzed (Figure 3). When 2 mm balls were used, the peak height after 60 min of grinding decreased to approximately 9% compared with the height prior to grinding.

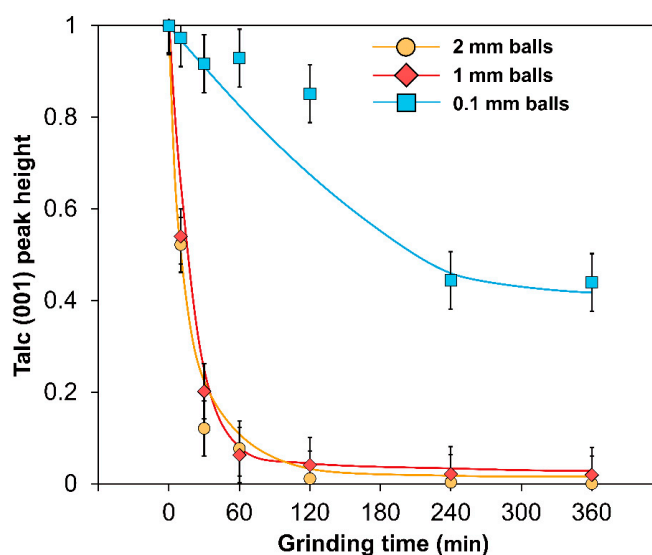


Figure 3. Changes in the relative intensities of (001) XRD peak of talc powder upon grinding with varying ball sizes for high-energy ball milling. The relative peak intensities are normalized with the (001) XRD peak of as-received talc.

Almost no peak was observed after 120 min of grinding. Similar results were obtained when 1 mm balls were used, but, after 120 min, the peak height decreased slightly to less than that obtained using 2 mm balls. When 0.1 mm balls were used, the peak height showed a slight decrease, and approximately 44% remained even after 360 min of grinding. These results indicate that the crystallinity of talc decreases more when 2 mm and 1 mm balls are used than when 0.1 mm balls are used for milling. As the ball size increases, greater size reduction of the talc particle and loss of crystallinity occur during grinding. This is due to the reduced kinetic energy of collision between rotating balls in the mill with 0.1 mm balls when compared with 2 mm and 1 mm balls [31,32].

Figure 4 shows the variation in relative peak intensities (I_t/I_0) of talc's main diffraction peaks such as (001), (132), (003), and (020) upon grinding, which shows the effect of the ball size on the direction in the fracture of talc. For 2 mm balls, the (001) and (003) lattice planes, which are perpendicular to the c-axis of talc, decreased faster than the (132) and (020) peaks. In particular, the decrease rate of (001) and (003) peaks was very high during the first 10 min and gradually slows at 60 min of grinding. The (001) and (003) peaks mostly disappeared after 120 min of grinding. In contrast, the decrease rate of the (132) and (020) peaks is relatively low and its peak intensities are approximately 20% after 360 min of grinding compared with that prior to grinding. The use of 1 mm balls yielded similar results to those obtained using 2 mm balls. The decrease rate of (001) and (003) peaks was very high in the early stage of grinding, and most of the peaks subsequently disappear. The (132) and (020) peak intensities are approximately 50% after 360 min of grinding when compared with that prior to grinding, which indicates less amorphization when using 1 mm balls than when using 2 mm balls.

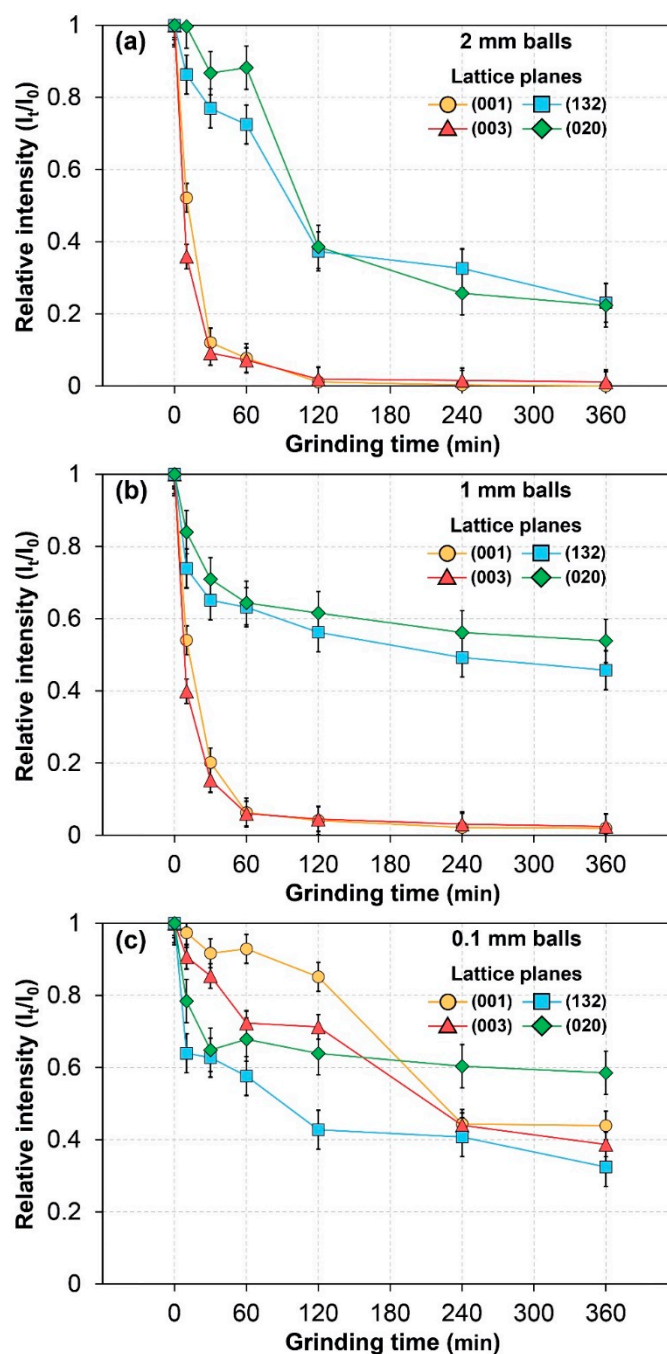


Figure 4. Effects of grinding time and ball size on the relative XRD intensities of lattice planes. The ball size for high-energy ball milling is (a) 2 mm, (b) 1 mm, and (c) 0.1 mm. The relative peak intensities are normalized with the XRD peak of as-received talc.

In contrast, when 0.1 mm balls were used, the decrease rate of (132) and (020) peaks was higher than that of the (001) and (003) peaks, especially during the first 60 min of grinding. After 360 min of grinding, all peaks except the (020) peak reached approximately 40% compared with that prior to grinding. As the ball size increases, the reduction of peak intensity prior to grinding increases for most peaks. The delamination of (001) planes, in particular, are significantly affected by the ball size. When 2 mm or 1 mm balls were used, the peak intensity of (001) planes reduced to less than 5% of its state prior to grinding, while it only reduced to 40% when using 0.1 mm balls. The relative intensities of (020) plane after 360 min of grinding were approximately 20%, 55%, and 60% when using 2 mm, 1 mm, and 0.1 mm balls, respectively. These results indicate that the size reduction mechanism of talc

changes with varying ball size. The contribution of delamination toward the decrease in particle size is high when 2 mm or 1 mm balls are used but low when 0.1 mm balls are used. The particle size reduction of talc occurred in all directions when using 0.1 mm balls.

3.2. Analysis of Specific Surface Area

Figure 5 shows the variation in the specific surface area of talc according to the ball size used in grinding.

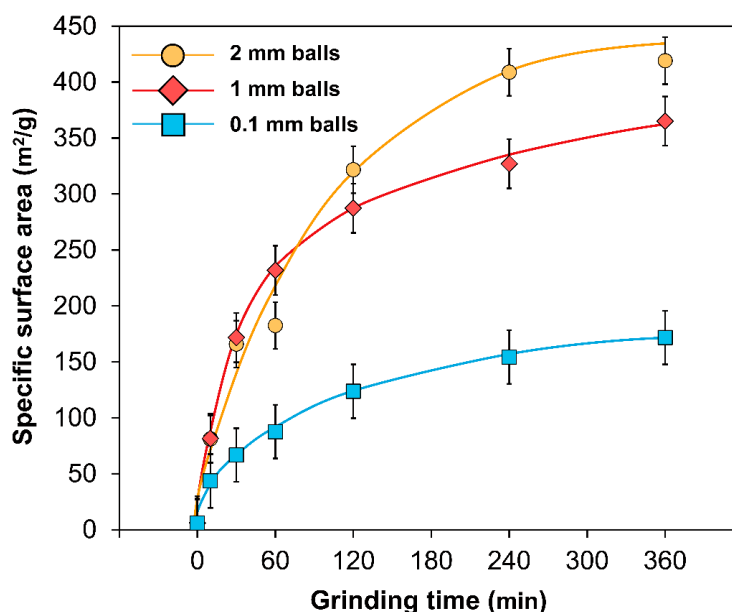


Figure 5. Variation of BET specific surface area of talc upon grinding with varying ball sizes for high-energy ball milling.

As the grinding progresses, the increase in the specific surface area of talc is initially abrupt and then becomes gradual. The overall tendency of the increase in the specific surface area is similar for all ball sizes. However, the degree of increase varied according to the ball size. When 2 mm or 1 mm balls were used, the tendency was very similar until 60 min of grinding. The specific surface area was slightly higher when 1 mm balls were used than when 2 mm balls were used. However, since the grinding time is increased above 60 min, the specific surface area of the particles ground using 2 mm balls increased more toward the end of the grinding period. The specific surface area was approximately 6.1 m²/g before grinding and increased to approximately 419.1 m²/g for 2 mm balls and approximately 365.1 m²/g for 1 mm balls after 360 min of grinding. The grinding efficiency when using 2 mm balls was slightly lower than when using 1 mm balls for the first 60 min of grinding, but prolonged grinding yielded a higher specific surface area when 2 mm balls were used. The 0.1 mm ball showed the lowest grinding efficiency, with a specific surface area of only 171.7 m²/g even after 360 min of grinding. These results indicate that the use of 1 mm and 2 mm balls in grinding talc could yield a larger specific surface area than the use of 0.1 mm balls could. In planetary ball milling, the proper ball size could maximize the grinding efficiency with a balance of aggregation and particle size reduction [32]. Our results indicate that the specific surface area eventually increases when the 2 mm balls are used for grinding, even though it is not clearly observed during the early stage of grinding.

The estimated spherical diameters (ESDs) were calculated using the equation $D = 6/\rho S$, where ρ is the density of talc (2.8 g/m³), S is the specific surface area (m²·g⁻¹), and the constant 6 is the shape factor assuming that the talc particles are spherical. The results are listed in Table 2.

Table 2. Changes in mineralogical parameters as a function of grinding time.

Talc	Ball Size (mm)	Grinding Time (min)						
		0	10	30	60	120	240	360
Relative (001) Peak height (%)	2		61.8	14.3	9.1	1.3	0.4	0.1
	1	100	63.9	23.9	7.2	4.7	2.3	2.2
	0.1		97.3	91.7	92.9	85.1	44.4	43.9
S _{BET} (m ² /g)	2		81.1	165.8	182.5	321.7	408.8	419.1
	1	6.1	81.5	171.6	231.8	287.3	326.9	365.1
	0.1		43.5	66.7	87.7	123.7	154.4	171.7
E.S.D. (nm)	2		26.4	12.9	11.7	6.7	5.2	5.1
	1	351.3	26.3	12.5	9.2	7.5	6.6	5.9
	0.1		49.3	32.1	24.4	17.3	13.9	12.5
Particle size (D ₅₀ , μm)	2		5.58	2.05	0.55	0.41	0.38	0.37
	1	12.8	3.25	0.71	0.52	0.45	0.41	0.44
	0.1		12.2	11.3	10.2	9.32	8.42	7.96

ESD, equivalent spherical diameter. $D = 6/\rho \cdot S$, where ρ is 2.8 g/cm³.

The powder had ESD of approximately 350 nm prior to grinding, which decreased to 5.1, 5.9, and 12.5 nm after 360 min of grinding using 2 mm, 1 mm, and 0.1 mm balls, respectively. These are much lower ESDs of talc than previously reported, as shown in Table 1 [10,14]. Data from previous reports listed in Table 1 were generally acquired under dry conditions, unlike the wet milling performed in this study.

We also obtained ground talc series with a similar specific surface area, even though the ball size varied. Similar specific surface areas of 81.1, 81.5, and 87.7 m²/g (approximately 85 m²/g) were obtained after 10 min of grinding with 2 mm and 1 mm balls and after 60 min of grinding with 0.1 mm balls, respectively. Furthermore, similar specific surface areas of 165.8, 171.6, and 171.7 m²/g (approximately 170 m²/g) were obtained after 30 min of grinding with 2 mm and 1 mm balls and after 360 min of grinding with 0.1 mm balls, respectively. These two series with a similar specific surface area will be discussed below.

3.3. Analysis of Particle Size by the Laser Diffraction Method

Figure 6 shows the evolution of the talc's particle size upon grinding, as measured by the laser diffraction particle size analysis.

The as-received talc shows a single distribution with a mean particle size of approximately 12 μm. With an increase in grinding time, the particle size generally decreased. However, the minimum particle size and reduction rate varied according to the ball size. When 2 mm and 1 mm balls were used, the particle size rapidly decreased to less than 1 μm for the first 60 min of grinding and did not change much after 120 min. However, when 0.1 mm balls were used, the particle size gradually decreases until 360 min of grinding, but the changes are relatively insignificant compared with the changes when using 1 mm and 2 mm balls.

The distribution pattern of particle sizes also varies upon grinding. The particle size of as-received talc shows a monomodal distribution ranging from ~3 to ~50 μm with a center at ~10 μm. As the grinding proceeds, an increase in submicron particles appeared in addition to the existing predominately micron-sized particles of approximately ~10 μm, which forms a bimodal distribution. In this case, we refer to the two distribution groups as a microscale group and a sub-microscale group. When using 1 mm and 2 mm balls, the sub-microscale group appears even after 10 min of grinding and its population gradually increases until 120 min of grinding at the expense of the microscale group. The mean particle size of the microscale group gradually decreases from ~10 to ~2 μm as the grinding proceeds for up to 60 min. The microscale group is not observed after 120 min of grinding, which indicates that talc powders are fully pulverized into sub-microscale after 120 min of grinding. However,

re-aggregation occurred in some samples, and, thus, small amounts of ~4 and ~20 μm particles were observed after 120 min of grinding. When using 0.1 mm balls, the population of the microscale group does not show a significant reduction even after 360 min of grinding and the population of the sub-microscale group is relatively insignificant when compared to the results when using 1 mm and 2 mm balls. We note that dispersion of the ground talc may be incomplete in aqueous solution and the sizes of the aggregated particles can be measured by the laser diffraction method.

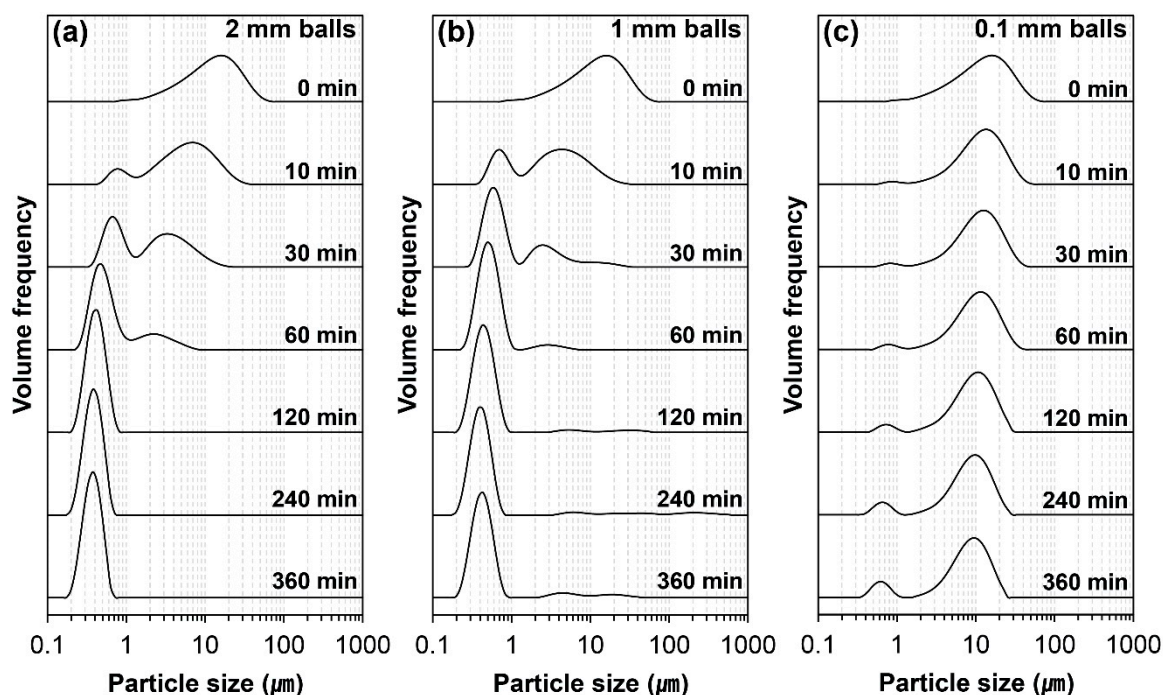


Figure 6. Changes in particle size of talc upon grinding, measured using laser diffraction particle size analysis. The ball size for high-energy ball milling is (a) 2 mm, (b) 1 mm, and (c) 0.1 mm.

Figure 7 shows the change in the D_{50} , which corresponds to 50% of the cumulative volume of the particle size distribution, upon grinding, according to the ball size.

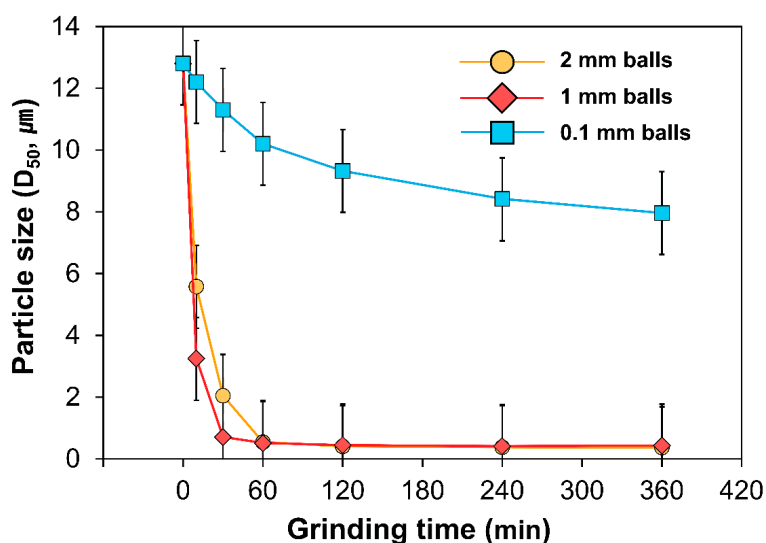


Figure 7. Change of particle size (D_{50}) of talc upon grinding.

When 2 mm balls were used, D_{50} decreased sharply to approximately 0.5 μm after 60 min of grinding, but did not show significant changes until 360 min. Similarly, when 1 mm balls were used, D_{50} decreased to approximately 0.7 μm in the first 30 min of grinding, but it did not change significantly after that. These results show that the particle size rarely decrease after approximately 60 min of grinding, which indicates that it reached the grinding limit under the grinding condition employed in this study. Until 60 min of grinding, the grinding efficiency of the 2 mm balls was slightly lower than that of the 1 mm balls. However, beyond this time frame, the D_{50} was smaller and the particle size distribution was narrower. In contrast, when 0.1 mm balls were used, the particle size steadily decreased until 360 min from the beginning of grinding. The final D_{50} was approximately 7.9 μm , which is approximately 7 μm larger than that obtained using 2 mm or 1 mm balls. These results indicate that, when 0.1 mm balls are used, the pulverization rate is slow and showed a lower grinding efficiency compared with the 2 mm and 1 mm balls.

3.4. Aggregation of Ground Talc

Laser diffraction particle size analysis and BET-specific surface area analysis are general methods to analyze the changes in particle size upon grinding. Though the calculated ESD based on the BET-specific surface area is much smaller than the results of particle size analysis because the shape of phyllosilicate talc and the increase in specific surface area generally indicates the decrease in particle size. According to the laser diffraction particle size analysis, the particle size of talc ground using 2 mm and 1 mm balls significantly decreased until 60 min of grinding, and further size reduction was not subsequently observed. On the contrary, BET-specific surface area continuously increases after 60 min of grinding. In addition, the significant difference in a specific surface area between talc powders ground using 2 mm and 1 mm balls is observed while the result of the particle size analysis shows only a trivial difference. These differences between the laser diffraction particle size and surface area analysis can appear when the ultrafine talc particles are aggregated by grinding [12]. In the BET-specific surface area analysis, there is a rare effect of aggregation because the N_2 gas is adsorbed to the particle surface. However, in the particle size analysis using laser diffraction, the size of aggregates can be measured rather than the individual particles. These results indicate that aggregation of ultrafine talc powder occurred as a result of grinding.

The aggregation of ground talc particles can be observed in SEM images of the talc particles grounded using 1 mm balls (Figure 8).

Before grinding, a unique laminar structure of talc is clearly observed with a size of tens of micrometers. With increasing grinding time, the particle size decreases to approximately 5 μm after 30 min, less than approximately 1 μm after 240 min, and approximately 200–300 nm after 360 min of grinding. The aggregation of ultrafine particles is clearly observed after 240 min of grinding, which is consistent with results of the laser diffraction particle size and BET-specific surface area analysis.

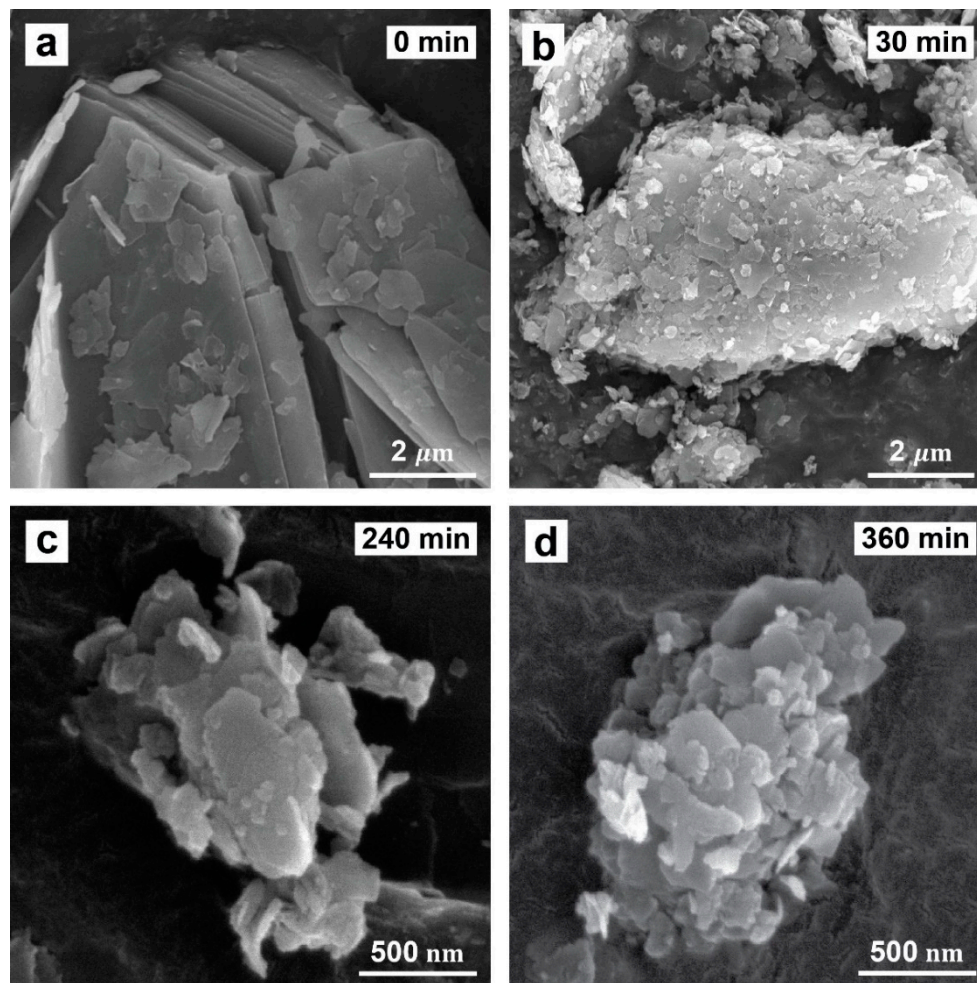


Figure 8. SEM images of ground talc for (a) 0 min, (b) 30 min, (c) 240 min, and (d) 360 min using 1 mm balls for high-energy ball milling.

In order to understand the effect of ball size on the aggregation of ground talc, Figure 9 compares the particle size analysis results of talc powders with similar specific surface areas. As described above, we obtain the ground talc series that have a similar specific surface area of talc particles that are approximately $85 \text{ m}^2/\text{g}$ and $170 \text{ m}^2/\text{g}$. The laser diffraction particle size of the ground talc using 2 mm and 1 mm balls showed similar particle size distribution when compared with the case of using 0.1 mm balls. In both series, the intensity of the sub-microscale group was larger when using 2 mm and 1 mm balls than when using 0.1 mm balls, which indicates a larger particle size when using 0.1 mm balls.

The different particle size distributions with similar surface area could be observed if the aggregation of ultrafine particles occurred as a result of grinding. The larger particle size distribution indicates the more aggregated status of talc powder. In this study, the ground talc powder using 0.1 mm balls shows a larger particle size than other talc powders with similar surface areas, which indicates that it is easily aggregated due to grinding.

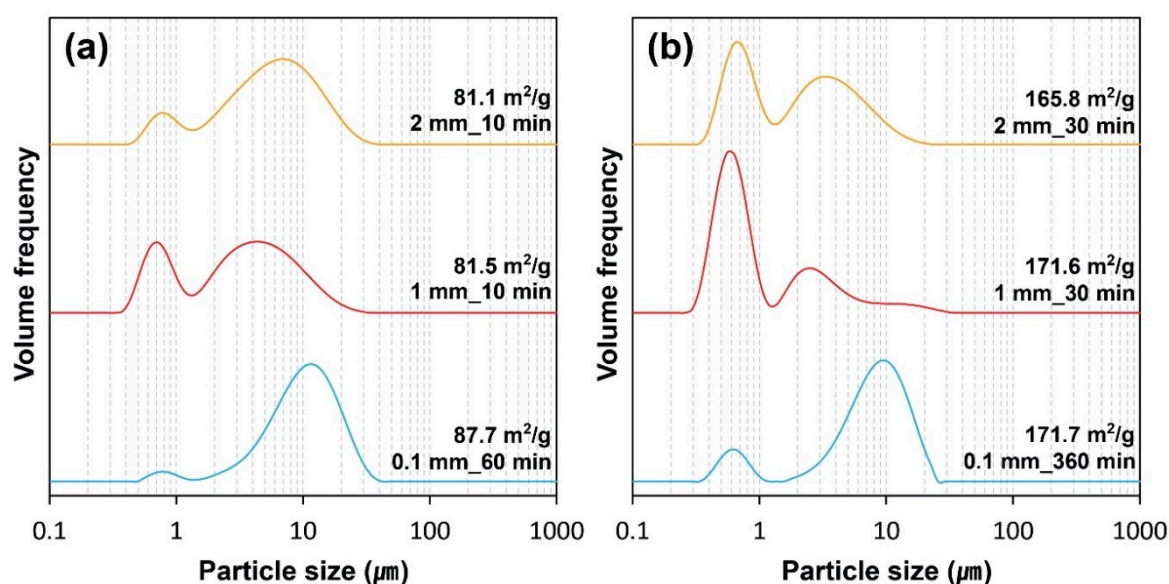


Figure 9. Comparison of particle size analysis results for ground talc powder having similar specific surface area. The BET specific surface areas are (a) 81–88 m²/g and (b) 165–172 m²/g.

The increased aggregation of ground talc with 0.1 mm balls than with 1 mm or 2 mm balls could be related to the degree of dispersion in the aqueous solution used in the particle size analysis. The aggregation of ultrafine particles generally occurs in order to reduce the high surface energy [34,35]. The talc powders with a similar surface area and different aggregation behavior indicate that these ground talc powders have a different surface energy and/or property. The results of XRD analysis showed that different crystallinity of ground talc powder depends on ball size. The crystallinity of ground talc is higher when using 0.1 mm balls than when using 1 mm and 2 mm balls. Crystalline talc is hydrophobic due to the siloxane sheet of the T-O-T layer. Hence, it aggregates well in aqueous solution [1,36]. On the other hand, disordered talc with lower crystallinity due to grinding is delaminated. Breakage of the layers exposes the hydroxyl groups in the octahedral layer. As a result, the talc is less hydrophobic due to the loss of crystallinity [8,37,38]. In an aqueous solution, the more hydrophilic talc is better dispersed.

As shown in Figure 3, the crystallinity of ground talc prepared using 0.1 mm balls during grinding is higher than that using 1 mm and 2 mm balls even though these talc powders have similar surface areas. The ground talc with relatively higher crystallinity (i.e., when using 0.1 mm balls for grinding) has higher surface energy than other ground talc powders (i.e., when using 1 mm and 2 mm balls for grinding). Thus, increased aggregation could occur in ground talc using 0.1 mm balls due to the loss of crystallinity and hydrophobicity.

4. Discussion

As described above, the grinding of talc using a high-energy ball mill results in differences in crystallinity, particle size, specific surface area, and aggregation behavior. Figure 10 shows the changes in the crystallinity, particle size, and specific surface area of talc, according to the ball size used in milling.

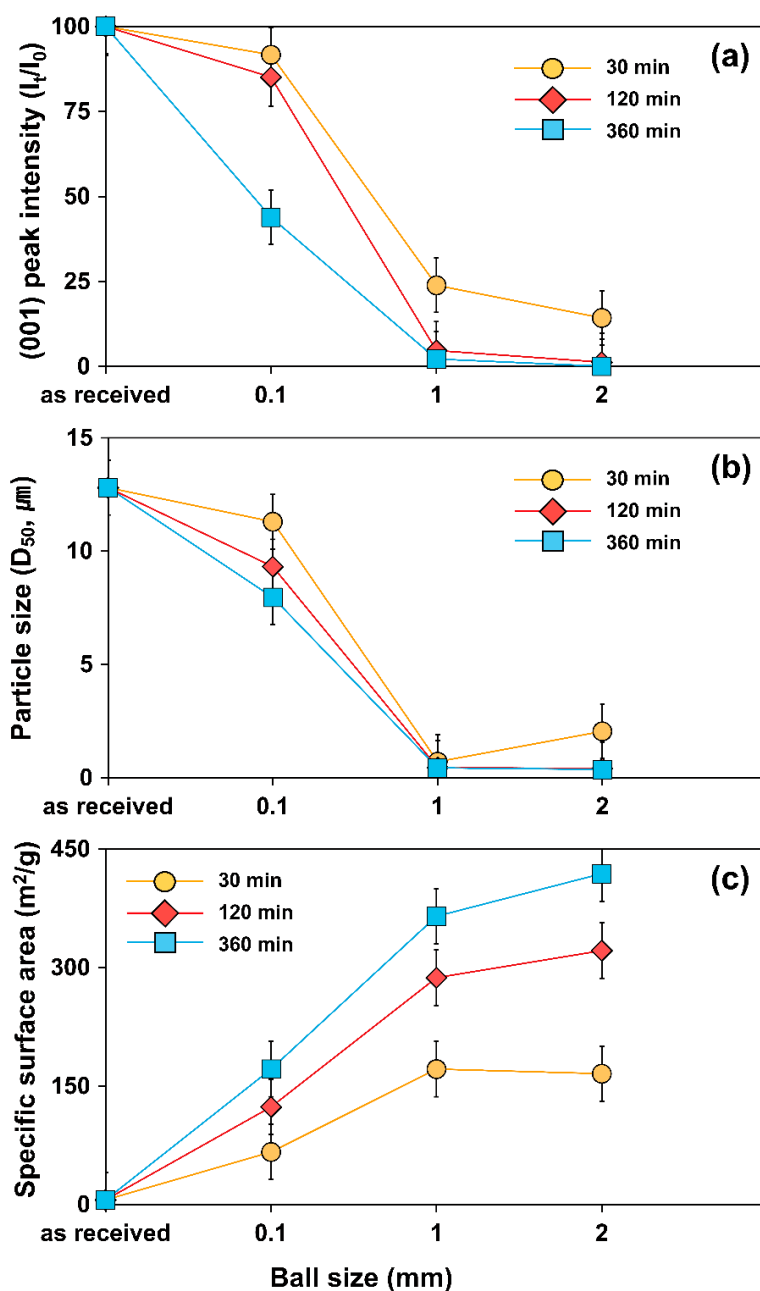


Figure 10. Effect of ball size for high-energy ball milling on (a) relative intensities of (001) XRD peak, (b) particle size (D_{50}), and (c) specific surface area.

4.1. Effects on Crystallinity of Ground Talc

The crystallinity of talc decreased upon grinding, and the degree of decrease varied depending on the ball size (Figure 10a). When 1 mm and 2 mm balls were used in grinding, the crystallinity decreased rapidly within 60 min of grinding, and delamination of (001) planes mainly occurred. After 120 min of grinding, almost all XRD peaks disappeared. In contrast, when grinding was performed using 0.1 mm balls, not only was there a reduction in the crystallinity decrease, but also crystal surfaces other than the (001) surface were fractured together. The crystallinity decreased continuously even after 120 min, but it was still much higher when compared with the case of using 1 mm and 2 mm balls. Compared with it prior to grinding, the (001) peak heights of XRD decreased to 91.7%, 23.9%, and 14.3% of the original size after 30 min of grinding when 0.1 mm, 1 mm, and 2 mm balls were used, respectively. After 120 min of grinding, it decreased to 85.1%, 4.7%, and 1.3%, respectively, and, after

360 min of grinding, it decreased to 43.9%, 2.2%, and 0.1%, respectively. When comparing the XRD patterns of ground talc with a similar specific surface area, the smaller the ball size used, the higher the final crystallinity of the talc is. These results indicate that the smaller ball size is appropriate to grind the talc while retaining the crystalline structure.

4.2. Effects on Comminution Rate and Limitation

The ball size in ball milling also affects the comminution rate and the limitation in particle size reduction. The increase in the comminution rate is clearly observed in the variation of particle size and BET-specific surface area, according to the ball size (Figure 10b,c). The BET-specific surface area of ground talc powders for 360 min shows approximately 419.1, 365.1, and 171.7 m²/g using 2 mm, 1 mm, and 0.1 mm sized balls, respectively. The ESD for those talc powders correspond to 5.1, 5.9, and 12.5 nm, respectively. The particle size measured by the laser diffraction method also corresponds to the submicroscale when using 1 mm and 2 mm balls, but to the microscale when using 0.1 mm balls after grinding for 360 min. According to the variation of BET-specific surface area, the comminution rate increased with increasing ball size. At the early stage of ball milling, the comminution rate difference between using 1 mm and 2 mm balls is insignificant. The comminution rate when using 1 mm balls is slightly faster than when using 2 mm balls at the early stage of grinding, but both the comminution rate and the limitation in particle size reduction are more effective when using 2 mm balls in prolonged grinding.

4.3. Effects on Aggregation

The ball size used in ball milling also affects the aggregation properties of talc. The larger the ball size used for grinding, the less aggregation occurred for talc powders with similar specific surface areas. When 1 mm and 2 mm balls were used, aggregates of submicron particles were formed in most cases, as observed in laser diffraction particle size analysis. However, when 0.1 mm balls were used, aggregates of several micron particles were formed, as shown in Figure 9. The differences between the particle size analysis and the specific surface area analysis would be caused by the formation of aggregates of the sample due to ongoing grinding. This means that, as the ball size increases, the aggregates are formed more easily. When talc powders with similar specific surface areas were compared, the smaller the ball size is, the larger the aggregates formed are. The aggregation behavior of ground talc varies with the ball size used during milling, which is the result of different talc crystallinities. The loss of talc crystallinity results in a loss of hydrophobicity [8,37,38] and, consequently, better dispersion in an aqueous solution. The ground talc exhibits more hydrophilic properties when larger balls are used during milling.

5. Conclusions

In this study, talc was ground at a fast rotation speed of 2000 rpm using a high-energy ball mill, and ultrafine talc particles were obtained. Furthermore, the effects of ball size on the grinding efficiency and crystallinity of talc were investigated. When a larger ball size was used in ball milling, the crystallinity decreased faster, and the grinding efficiency and the specific surface area of the talc increased. In the case of crystallinity, the smaller the ball size was, the smaller the decrease in crystallinity was. Therefore, using a small ball size can produce talc nanoparticles with higher crystallinity. Upon the progress of milling, the aggregation of talc particles occurs and the degree of aggregation shows the relations with crystallinity of talc. Comparing the ground talc with similar specific surface areas, the more disordered the structure of the ground talc is, the fewer aggregation and more hydrophilic properties are observed.

Author Contributions: Conceptualization, H.N.K. Validation, J.W.K. and M.S.K. Investigation, H.N.K., J.W.K., M.S.K., B.H.L. and J.C.K. Writing—original draft preparation, H.N.K. and J.W.K. Writing—review and editing, H.N.K. Visualization, J.W.K. and M.S.K. Project administration, H.N.K. Funding acquisition, H.N.K. Please turn to the CRediT taxonomy for the term explanation.

Funding: The National Research Foundation of Korea (grant number NRF-2016R1C1B1010108) supported this work and the “Human Resources Program in Energy Technology” of the Korea Institute of Energy Technology Evaluation and Planning (KETEP) granted financial resources from the Ministry of Trade, Industry & Energy, Republic of Korea (grant number 20194010201730).

Conflicts of Interest: The authors declare no conflict of interest.

References

1. Brigatti, M.F.; Galan, E.; Theng, B.K.G. Structures and mineralogy of clay minerals. In *Developments in Clay Science*; Bergaya, F., Theng, B.K.G., Lagaly, G., Eds.; Elsevier: Amsterdam, The Netherlands, 2006; Volume 1, pp. 19–86.
2. Zazenski, R.; Ashton, W.H.; Briggs, D.; Chudkowski, M.; Kelse, J.W.; Maceachern, L.; McCarthy, E.F.; Nordhauser, M.A.; Roddy, M.T.; Teetsel, N.M.; et al. Talc: Occurrence, characterization, and consumer applications. *Regul. Toxicol. Pharmacol.* **1995**, *21*, 218–229. [[CrossRef](#)] [[PubMed](#)]
3. Castillo, L.; López, O.; López, C.; Zaritzky, N.; García, M.A.; Barbosa, S.; Villar, M. Thermoplastic starch films reinforced with talc nanoparticles. *Carbohydr. Polym.* **2013**, *95*, 664–674. [[CrossRef](#)]
4. Maiti, S. Mechanical, morphological, and thermal properties of nanotalc reinforced PA6/SEBS-g-MA composites. *J. Appl. Polym. Sci.* **2015**, *132*. [[CrossRef](#)]
5. Elfaki, H.; Hawari, A.; Mulligan, C. Enhancement of multi-media filter performance using talc as a new filter aid material: Mechanistic study. *J. Ind. Eng. Chem.* **2015**, *24*, 71–78. [[CrossRef](#)]
6. Galet, L.; Goalard, C.; Dodds, J.A. The importance of surface energy in the dispersion behaviour of talc particles in aqueous media. *Powder Technol.* **2009**, *190*, 242–246. [[CrossRef](#)]
7. Kim, J.W.; Lee, B.H.; Kim, J.C.; Kim, H.N. Particle size analysis of nano-sized talc prepared by mechanical milling using high-energy ball mill. *J. Mineral. Soc. Korea* **2018**, *31*, 47–55. [[CrossRef](#)]
8. Caban-Nevarez, R.; Perez, O.J.P. Size-dependence hydrophobicity in nanocrystalline talc produced by high-intensity planetary ball milling. *MRS Online Proc. Libr. Arch.* **2015**, 1805. [[CrossRef](#)]
9. Dumas, A.; Claverie, M.; Slostowski, C.; Aubert, G.; Careme, C.; Le Roux, C.; Micoud, P.; Martin, F.; Aymonier, C. Fast-geomimicking using chemistry in supercritical water. *Angew. Chem. Int. Ed.* **2016**, *55*, 9868–9871. [[CrossRef](#)]
10. Dellisanti, F.; Minguzzi, V.; Valdrè, G. Mechanical and thermal properties of a nanopowder talc compound produced by controlled ball milling. *J. Nanopart. Res.* **2011**, *13*, 5919–5926. [[CrossRef](#)]
11. Kano, J.; Saito, F. Correlation of powder characteristics of talc during planetary ball milling with the impact energy of the balls simulated by the particle element method. *Powder Technol.* **1998**, *98*, 166–170. [[CrossRef](#)]
12. Dellisanti, F.; Valdrè, G.; Mondonico, M. Changes of the main physical and technological properties of talc due to mechanical strain. *Appl. Clay Sci.* **2009**, *42*, 398–404. [[CrossRef](#)]
13. Filio, J.M.; Sugiyama, K.; Saito, F.; Waseda, Y. A study on talc ground by tumbling and planetary ball mills. *Powder Technol.* **1994**, *78*, 121–127. [[CrossRef](#)]
14. Sanchez-Soto, P.J.; Wiewióra, A.; Avilés, M.A.; Justo, A.; Pérez-Maqueda, L.A.; Pérez-Rodríguez, J.L.; Bylina, P. Talc from Puebla de Lillo, Spain. II. Effect of dry grinding on particle size and shape. *Appl. Clay Sci.* **1997**, *12*, 297–312. [[CrossRef](#)]
15. Borges, R.; Macedo Dutra, L.; Barison, A.; Wypych, F. MAS NMR and EPR study of structural changes in talc and montmorillonite induced by grinding. *Clay Miner.* **2016**, *51*, 69–80. [[CrossRef](#)]
16. Cayirli, S. Dry grinding of talc in a stirred ball mill. *EDP Sci.* **2016**, *8*, 01005–01013. [[CrossRef](#)]
17. Sakthivel, S.; Pitchumani, B. Production of nano talc material and its applicability as filler in polymeric nanocomposites. *Part. Sci. Technol.* **2011**, *29*, 441–449. [[CrossRef](#)]
18. Čavajda, V.; Uhlík, P.; Derkowski, A.; Čaplovičová, M.; Madejová, J.; Mikula, M.; Ifka, T. Influence of grinding and sonication on the crystal structure of talc. *Clays Clay Miner.* **2015**, *63*, 311–327. [[CrossRef](#)]
19. Christidis, G.; Makri, P.; Perdikatsis, V. Influence of grinding on the structure and colour properties of talc, bentonite and calcite white fillers. *Clay Miner.* **2004**, *39*, 163–175. [[CrossRef](#)]
20. Kano, J.; Miyazaki, M.; Saito, F. Ball mill simulation and powder characteristics of ground talc in various types of mill. *Adv. Powder Technol.* **2000**, *11*, 333–342. [[CrossRef](#)]
21. Ohenoja, K.; Illikainen, M. Effect of operational parameters and stress energies on stirred media milling of talc. *Powder Technol.* **2015**, *283*, 254–259. [[CrossRef](#)]

22. Cook, T.M.; Courtney, T.H. The effects of ball size distribution on attritor efficiency. *Metall. Mater. Trans. A* **1995**, *26*, 2389–2397. [[CrossRef](#)]
23. Choi, W.S.; Chung, H.Y.; Yoon, B.R.; Kim, S.S. Applications of grinding kinetics analysis to fine grinding characteristics of some inorganic materials using a composite grinding media by planetary ball mill. *Powder Technol.* **2001**, *115*, 209–214. [[CrossRef](#)]
24. Lameck, N.N.S. Effects of Grinding Media Shapes on Ball Mill Performance. Master's Dissertation, University of the Witwatersrand, Johannesburg, South Africa, 2006.
25. Katubilwa, F.M.; Moys, M.H. Effect of ball size distribution on milling rate. *Miner. Eng.* **2009**, *22*, 1283–1288. [[CrossRef](#)]
26. Mio, H.; Kano, J.; Saito, F.; Kaneko, K. Effects of rotational direction and rotation-to-revolution speed ratio in planetary ball milling. *Mater. Sci. Eng. A* **2002**, *332*, 75–80. [[CrossRef](#)]
27. Liao, J.; Senna, M. Thermal behavior of mechanically amorphized talc. *Thermochim. Acta* **1992**, *197*, 295–306. [[CrossRef](#)]
28. Filippov, L.O.; Joussemet, R.; Irannajad, M.; Houot, R.; Thomas, A. An approach of the whiteness quantification of crushed and floated talc concentrate. *Powder Technol.* **1999**, *105*, 106–112. [[CrossRef](#)]
29. Yekeler, M.; Ulusoy, U.; Hiçyılmaz, C. Effect of particle shape and roughness of talc mineral ground by different mills on the wettability and floatability. *Powder Technol.* **2004**, *140*, 68–78. [[CrossRef](#)]
30. Faraji, G.; Kim, H.S.; Kashi, H.T. *Severe Plastic Deformation: Methods, Processing and Properties*; Elsevier: Amsterdam, The Netherlands, 2018.
31. Akçay, K.; Sirkecioğlu, A.; Tatlıer, M.; Savaşçı, Ö.T.; Erdem-Şenatalar, A. Wet ball milling of zeolite HY. *Powder Technol.* **2004**, *142*, 121–128. [[CrossRef](#)]
32. Shin, H.; Lee, S.; Suk Jung, H.; Kim, J.-B. Effect of ball size and powder loading on the milling efficiency of a laboratory-scale wet ball mill. *Ceram. Int.* **2013**, *39*, 8963–8968. [[CrossRef](#)]
33. Boulvais, P.; de Parseval, P.; D'Hulst, A.; Paris, P. Carbonate alteration associated with talc-chlorite mineralization in the eastern Pyrenees, with emphasis on the St. Barthelemy Massif. *Mineral. Petrol.* **2006**, *88*, 499–526. [[CrossRef](#)]
34. Jung, S.J.; Lutz, T.; Boese, M.; Holmes, J.D.; Boland, J.J. Surface energy driven agglomeration and growth of single crystal metal wires. *Nano Lett.* **2011**, *11*, 1294–1299. [[CrossRef](#)] [[PubMed](#)]
35. Thielmann, F.; Naderi, M.; Ansari, M.A.; Stepanek, F. The effect of primary particle surface energy on agglomeration rate in fluidised bed wet granulation. *Powder Technol.* **2008**, *181*, 160–168. [[CrossRef](#)]
36. Yi, H.; Zhao, Y.; Rao, F.; Song, S. Hydrophobic agglomeration of talc fines in aqueous suspensions. *Colloids Surf. A Physicochem. Eng. Asp.* **2018**, *538*, 327–332. [[CrossRef](#)]
37. Zbik, M.; Smart, R.S.C. Influence of dry grinding on talc and kaolinite morphology: Inhibition of nano-bubble formation and improved dispersion. *Miner. Eng.* **2005**, *18*, 969–976. [[CrossRef](#)]
38. Kim, M.S.; Kim, J.W.; Kang, C.D.; So, B.D.; Kim, H.N. Variation of water content and thermal behavior of talc upon grinding: Effect of repeated slip on fault weakening. *J. Miner. Soc. Korea* **2019**, *32*, 201–211. [[CrossRef](#)]

